Arabian Journal of Chemistry (2021) **14**, 103179

King Saud University

Arabian Journal of Chemistry

www.ksu.edu.sa
www.sciencedirect.com

ORIGINAL ARTICLE

A multidisciplinary study of chemico-physical properties of different classes of 2-aryl-5(or 6)-nitrobenzimidazoles: NMR, electrochemical behavior, ESR, and DFT calculations

El Mostapha Rakib [a], Carla Boga [b], Matteo Calvaresi [c], Mohamed Chigr [a], Paola Franchi [c], Isacco Gualandi [b], Aziz Ihammi [a], Marco Lucarini [c], Gabriele Micheletti [b,*], Domenico Spinelli [c,*], Domenica Tonelli [b]

[a] *Laboratory of Organic and Analytic Chemistry, Faculty of Sciences and Technics, Sultan Moulay Slimane University, BP 523, 2300 Beni-Mellal, Morocco*
[b] *Department of Industrial Chemistry 'Toso Montanari' Alma Mater Studiorum, Università di Bologna, Viale del Risorgimento 4, Bologna 40136, Italy*
[c] *Department of Chemistry 'G. Ciamician' Alma Mater Studiorum, Università di Bologna, Via Selmi 2, Bologna 40126, Italy*

Received 9 February 2021; accepted 18 April 2021
Available online 26 April 2021

KEYWORDS

2-Aryl-nitrobenzimidazoles;
^{1}H and ^{13}C NMR;
Cyclic voltammetry;
Electron spin resonance;
DFT calculations

Abstract Continuing in our researches on the syntheses, reactivity, pharmacological/biological activities of heterocyclic compounds containing one or more nitrogen atoms we have examined some chemico-physical properties (^{1}H and ^{13}C NMR, electrochemical behavior, and ESR) of three series of 2-aryl-5(or 6)-nitrobenzimidazoles (**1**–**3**) variously substituted in the 2-aryl ring. The electrochemical behavior of the nitro group on the benzimidazole ring has been studied by cyclic voltammetry. This has allowed to point out both the reversibility, the formal potential, and the number of electrons involved in the electrochemical processes, and to evaluate the effect of the substituents present on the aryl ring. The data collected have been able to furnish a complete picture of electronic distribution and have been supported by DFT calculations.

1. Introduction

Benzocondensed imidazole represents an interesting substrate characterized by a high degree of aromaticity (aromatic index for benzimidazole: 146 according with Bird's classification) (Bird, 1992). It and its derivatives show a variegated chemical

* Corresponding authors.
E-mail addresses: gabriele.micheletti3@unibo.it (G. Micheletti), domenico.spinelli@unibo.it (D. Spinelli).
Peer review under responsibility of King Saud University.

ELSEVIER Production and hosting by Elsevier

https://doi.org/10.1016/j.arabjc.2021.103179

reactivity and several of them present potential pharmacological activities (Marinescu, 2019).

Therefore, they have attracted significant attention because of some important biological and pharmacological properties (Bansal and Silakari, 2012; Bhattacharya and Chaudhuri, 2008). In fact, they are widely used as drugs in anticancer (El-Karim et al., 2018; Shaharyar et al., 2010; Thimmegowda et al., 2008), antiviral (Starcevic et al., 2007), antibacterial (Desai and Desai, 2006; El-Gohary and Shaaban, 2017; Guven, 2007; Kahveci et al., 2014; Pathan and Rahatgaonkar, 2016; Romagnoli et al., 2017; Shahid et al., 2016; Vijesh et al., 2013), antihypertensive (Jain et al., 2013; Kubo et al., 1993), antihelminthic (Mavrova et al., 2006), antiprotozoal (Perez-Viaòònueva et al., 2013), anti-inflammatory (Gaba et al, 2010; Sondhi et al., 2006), antifungal, (Madkour et al., 2006), and antitubercular (Kalalbandi et al., 2014; Pieroni et al., 2011) treatments. Furthermore, benzimidazole derivatives are also effective against HIV (Morningstar et al., 2007) and human cytomegalovirus (HCMV) (Zhu et al. 2000). Derivatives of benzimidazole variously decorated with different substituents (essentially at C-2, but also in the benzene ring) are among the most important nitrogen-containing heterocycles, widely explored and utilized by the pharmaceutical industry for drug discovery (Fig. 1) (Hadole et al., 2018).

Recently, several papers have been published reporting the syntheses of these heterocyclic compounds in different experimental conditions: for example, solvent free or using reactant immobilized on solid support, microwave irradiation condition, in different solvents and using various catalysts (Das et al., 2018; Largeron and Nguyen, 2018). The classical approach to synthesize benzimidazole derivatives is the condensation of 1,2-phenylenediamine with carboxylic acids or their derivatives under strong acidic conditions (Panda et al., 2012; Preston, 1981). Another widely used strategy involves the condensation of 1,2-phenylenediamine with aldehydes/alcohols in the presence of different oxidizing agents (Bahrami et al., 2007; Beaulieu et al., 2003; Chen et al., 2008; Sthephens and Bower, 1949).

In this line, following previous experience in the field, our composite research group, collecting people with different competences, from the study of the synthesis and the chemical reactivity (Bianchi et al., 2006; Boga et al., 2016a; D'Anna et al., 2006; Dell'Erba and Spinelli, 1965; Frenna et al., 2019; Micheletti et al, 2019; Spinelli et al., 1972, 1975) as well as the biological properties (Budriesi et al., 2002; Carosati et al., 2016; Cuviello et al., 2019; Rosano et al., 2013; Viale et al., 2009) of heterocyclic compounds (containing nitrogen, sulphur and/or oxygen atoms) to the study of their NMR properties (Boga et al., 2016b; Dell'Erba et al., 1990; Delpivo et al., 2013; Del Vecchio et al., 2015; Micheletti et al., 2016; Spinelli and Zanirato, 1993) and from the examination of electrochemical voltammetric data to those of electron spin resonance have joined their expertise to carry out a research on several nitrobenzimidazoles with the aim of gaining information on their electronic distribution and then on their possible chemical/biological behavior. To extend the global vision of the studied compounds we have also carried DFT calculations useful to gain information on the different stability of the possible tautomers and on the nature of the possible interactions between the chemical groups present in the studied molecules surely so gaining useful information about the electronic density on the various atoms of the studied molecules and then on their reactivity (Boga et al., 2012; Micheletti et al., 2017; Kouakou et al., 2015).

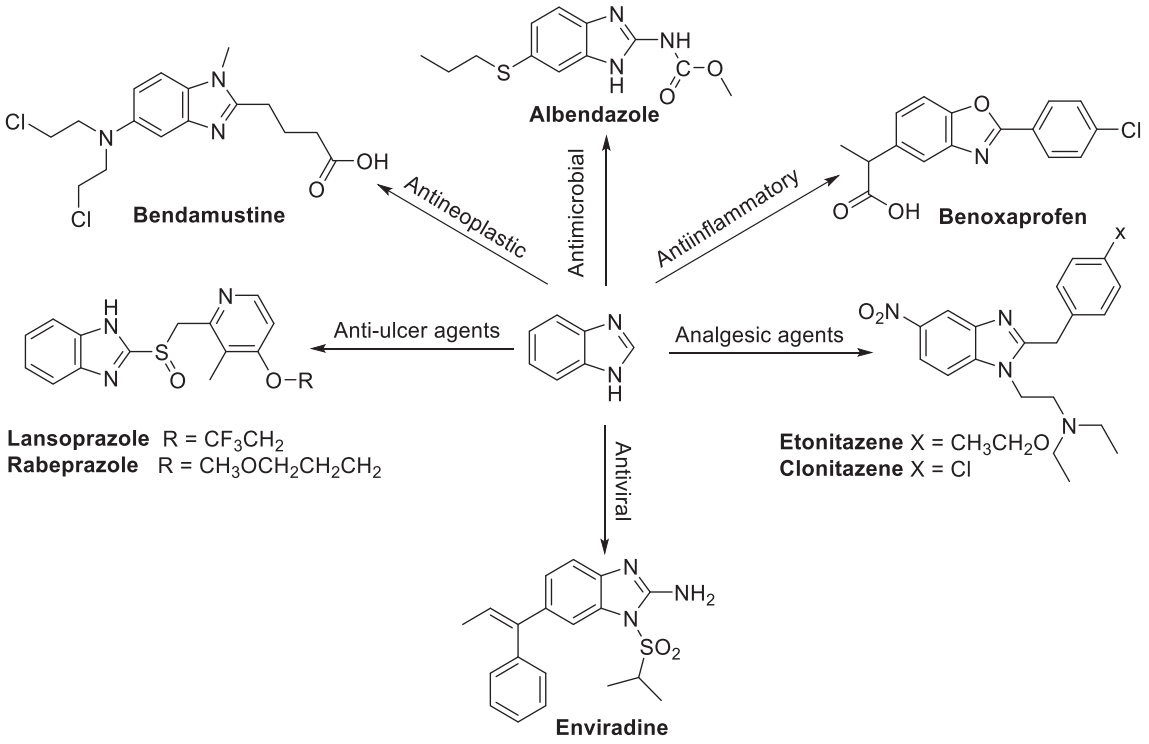

Fig. 1 Pharmacological properties of different drugs deriving from benzimidazole.

Thus, we have now addressed our attention to a lot of derivatives (1–3) of 5(or 6)-nitrobenzimidazole substituted at C-2 with an aryl group and, eventually, at a nitrogen atom of the imidazole ring with a methyl group.

2-Aryl-5-(or 6)-nitrobenzimidazoles (1a-f) give rise to a 'tautomeric' equilibrium (Scheme 1), able to affect electronic distribution, stability, and reactivity of the examined substrates.

In 1-methyl-2-aryl-5-nitrobenzimidazoles (2a-f) and in 1-methyl-2-aryl-6-nitrobenzimidazoles (3a-f), two 'isomers' (Fig. 2), different interactions between the nitro group and the nitrogen atoms of the imidazole ring could be operating.

In all the three series of benzimidazoles different conjugative interactions are operating. We think that the most important is that one between the two nitrogen atoms of the imidazole ring: one 'pyrrole-like' and the other 'pyridine-like': in series **1** it is the 'motor' of the tautomerism. Looking at the **1B** tautomer a conjugative long-range interaction between the pyrrole-like nitrogen and the nitro group can occur, while a *para*-like interaction can happen in the **1A** tautomer. Moreover, looking at compounds **2** one can observe that in *para*-position with respect to the nitro group at C-5 a 'pyrrole-like' nitrogen is present (probably able to interact donating electrons), instead in compounds **3** a 'pyridine-like' nitrogen is present (probably able to interact attracting electrons). These two different possible electronic interactions could be able to affect in a different manner the chemico-physical behavior of this nitro group.

All of the three classes of nitrobenzimidazoles (**1–3**) contain at C-2 a phenyl group variously substituted (X = H, 3′-Br, 4′-F, 4′-Cl, 4′-NMe2, 4′-NO2) that is they hold substituents with very different electronic characters (Hansch and Leo, 1979) from the strong electron-donating dimethylamino group (σ_p-0.83, σ_p^--1.7) to the strong electron-attracting nitrogroup (σ_p + 0.78, σ_p^+ +1.27), then able to variously affect the electronic density in compounds **1–3**.

Moreover, we suppose that compounds **1f**, **2f**, and **3f** could be of special interest, because the nitro group present in the phenyl group could be able to compete with the nitrogroup present on the condensed benzene ring in the interaction with electrons in both electrochemical and electron spin resonance processes.

2. Material and methods

2.1. General

NMR spectra were recorded at 600 and 150.80 MHz for ^{1}H NMR and ^{13}C NMR, respectively. *J* values are given in Hz.

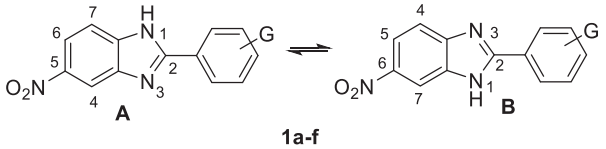

1a-f

G = H (**a**), 3-Br (**b**), 4-F (**c**),4-Cl (**d**), 4-N(CH$_3$)$_2$ (**e**), 4-NO$_2$ (**f**)

Scheme 1 Equilibrium in 2-aryl-5 (or 6)-nitrobenzimidazoles 1a-f.

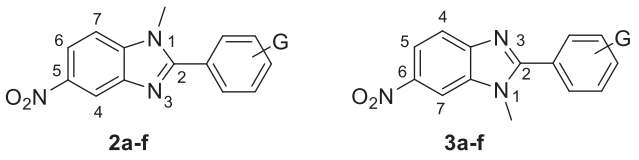

2a-f **3a-f**

G = H (**a**), 3-Br (**b**), 4-F (**c**),4-Cl (**d**), 4-N(CH$_3$)$_2$ (**e**), 4-NO$_2$ (**f**)

Fig. 2 Structure of 1-methyl-2-aryl-5-nitrobenzimidazoles (2a-f) and 1-methyl-2-aryl-6-nitrobenzimidazoles (3a-f).

Signal multiplicities were established by DEPT experiments. Signals assignment was made by the aid of NOESY, HSQC and HMBC experiments. Chemical shifts were measured in δ (ppm) with reference to the solvent [(δ = 2.50 and 39.5 ppm for DMSO d_6), (δ = 2.2 and 30.2 ppm for acetone d_6) for ^{1}H and ^{13}C NMR, respectively]. Variable temperature NMR and 2D low-temperature spectra were recorded on an instrument equipped with a direct PFG Probe. The temperatures were calibrated by substituting the sample with a precision Cu/Ni thermocouple before the measurements.

ESR spectra were recorded at room temperature using an ELEXYS E500 spectrometer equipped with a NMR gaussmeter for the calibration of the magnetic field and a frequency counter for the determination of *g*-factors that were corrected against that of the perylene radical cation in concentrated sulfuric acid (g = 2.002583). The electrochemical cell was homemade and consisted of an ESR flat cell (Wilmad WG-810) equipped with a 25 × 5 × 0.2 mm platinum gauze (cathode) and a platinum wire (anode). The current was supplied and controlled by an AMEL 2051 general-purpose potentiostat (Alberti et al., 2000; Boga et al., 2012; Kouakou, et al., 2015; Micheletti et al., 2017). In a typical experiment, the cell was filled with an acetonitrile (ACN) solution of the appropriate substrate (*ca.* 1 mM) containing tetrabutylammonium perchlorate (*ca.* 0.1 M) as supporting electrolyte. After thoroughly purging the solution with N_2, spectra were recorded at different potential settings in the range 0 to −3.0 V. An iterative least squares fitting procedure based on the systematic application of the Monte Carlo method was performed in order to obtain the experimental spectral parameters of the radical species (Gualandi et al., 2016).

Cyclic voltammetry (CV) measurements were performed under nitrogen atmosphere at room temperature in ACN (Chromanorm Prolabo, HPLC grade, freshly distilled over CaH_2) solution containing 0.1 M tetrabutylammonium hexafluorophosphate ($TBAPF_6$) as supporting electrolyte. The concentration of the compounds under investigation was about 2 mM. The CVs were recorded using a CHI 660c (CH Instruments, Austin, Texas) potentiostat controlled by a personal computer via CH Instruments original software, enabling the solution resistance compensation option. A single compartment, three electrode cell was employed. The working electrode was a GC disk (3 mm diameter) (from BASi, West Lafayette, Indiana), and the counter electrode was a Pt wire. As reference was used a Ag^+/Ag electrode, made of a silver wire immersed in a solution of 0.1 M $AgNO_3$ and 0.1 M $TBAPF_6$ in distilled ACN, and an external junction containing 0.1 M $TBAPF_6$ in distilled ACN so that to hinder Ag^+ release in the working solution. The potential of the reference electrode was checked daily by performing a CV in a solution of

2 mM ferrocene in the same electrolyte and solvent employed for all measurements. All potentials throughout the paper are reported *versus* ferrocinium/ferrocene couple. Prior to experiments the surface of the GC working electrode was polished first on a wet fine sandpaper (4000 grid), thoroughly rinsing the electrode surface firstly with distilled water and then with acetone. Finally, the working electrode was accurately dried. The cyclic voltammograms were recorded at different scan rates, from 0.010 to 20 V s^{-1} in both the cathodic and anodic regions.

All the computations reported herein were performed with the Gaussian16 (Frisch et al., 2016) series of programs. The geometry of the various stationary points was fully optimized with the gradient method available in Gaussian 16 at the DFT level using the nonlocal hybrid Becke's three-parameter exchange functional denoted as B3LYP (Becke, 1993; Lee, 1988) and the 6-311 + + G(d,p) basis set (Frisch et al., 1984). A computation of the harmonic vibrational frequencies was carried out to confirm the nature of each critical point. Isosurfaces spin densities were plotted using an isovalue of 0.004 $e\ a_0^{-3}$ using the software GaussView 6.

The general procedures concerning the syntheses of compounds 1–3, together with their physical properties, are reported in Supplementary Information.

3. Results and discussion

3.1. NMR studies

In NMR studies, to make easier the comparison of data, we adopted a unique '*conventional*' numbering for all compounds, as reported in Fig. 3.

The assignment of the signals was made, in some cases, with the aid of NOESY experiments to identify protons in proximity of *N*-methyl groups, and 2D experiments to assign the CH carbons (HMQC) as well as the quaternary carbons C3a and C7a (HMBC).

Below we report and discuss the results obtained, divided in sub-headings.

3.1.1. ^{1}H NMR data for benzimidazole derivatives *1a–f, 2a–f, and 3a–f*

In ^{1}H NMR spectra of NH-benzimidazole derivatives **1a**–**f**, recorded in DMSO d_6 at 25 °C, the signals due to NH, H-4, and H-7 resonances appeared broad, whereas the H-7 and H-4 of the corresponding *N*-methyl derivatives were always sharp. This behavior was likely due to the N-1/N-3 prototropic process on the imidazole ring (Scheme 1) that is not slow enough to give separate signals for the two tautomers, despite that the spectra are recorded in DMSO d_6, a solvent known to slow down the prototropic exchanges (Claramunt et al., 2006; Niet et al., 2014). At the same time, the interconversion process between the two tautomeric forms is not fast enough to make sharp all the signals averaged out on the NMR time-scale.

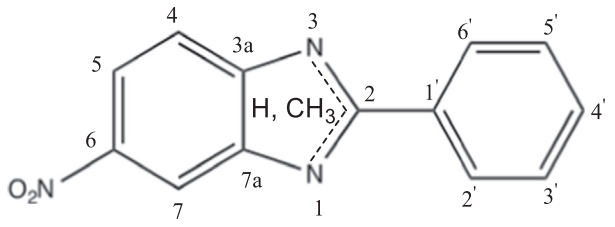

Fig. 3 Numbering adopted in describing NMR data for all compounds considered.

With the aim to reduce the line broadening observed as consequence of an average of exchanging states, we recorded the spectra in DMSO d_6 at 102 °C. Under these conditions, being the interconversion process faster than at 25 °C, all the ^{1}H NMR signals sharpened. In Table S1 in Supplementary Information are collected ^{1}H NMR data for NH-benzimidazole derivatives **1a**–**f**.

As expected, the only remarkable differences are found on the signals of the aryl substituent, in particular H-3′/H-5′ that are strongly affected by the presence of the substituent in *para* position. In the cases of *p*-*N*,*N*-dimethylamino (**1e**) and *p*-nitro derivative (**1f**) the H-3′/H-5′ chemical shifts are shifted of about 1 ppm highfield and downfield, respectively, with respect to the signals of **1a**.

The ^{1}H NMR data for 1-methyl-5-nitrobenzimidazoles **2a**–**f** and 1-methyl-6-nitrobenzimidazoles **3a**–**f** (Fig. 2), recorded in DMSO d_6 at 25 °C, are reported in Tables S2 and S3, respectively. A comparison of data in Tables S2 and S3 shows negligible variations of the chemical shifts between the two isomers. Only a slight low field shift (~0.1 ppm) for H-7 in 1-methyl-6-nitrobenzimidazoles and H-5 in 1-methyl-5-nitrobenzimidazoles is observed with respect to that of the other isomer.

3.1.2. ^{13}C NMR data for benzimidazole derivatives *1a–f, 2a–f, and 3a–f*

In the instance of NH-benzimidazole derivatives **1a**–**f**, the ^{13}C NMR spectra, recorded in DMSO d_6 at 25 °C, showed broad signals, as observed also in ^{1}H NMR spectra. It is known that when prototropic tautomerism occurs in NH-benzimidazoles, very commonly the signals of the benzimidazole carbons atoms coalesce in groups of two in an averaged signal (Claramunt et al., 2006; Niet et al., 2014).

Consequently, in the current study, with the aim to make faster the interconversion process between the two tautomeric forms (**A** and **B** of Scheme 1), ^{13}C NMR spectra have been recorded at 102 °C and the chemical shifts of the average signals are reported in Table S4. Nevertheless, in some cases, the ^{13}C NMR spectra presented again broad signals for C-4, C-6, C-3a and C-7a, making difficult the assignment.

^{13}C NMR data for 1-methyl-5-nitro- benzimidazoles **2a**–**f** and 1-methyl-6-nitro- benzimidazoles **3a**–**f** are reported in Tables S5 and S6, respectively.

The comparison of the chemical shifts along each series (**2** and **3**) was based on the differences of chemical shifts (reported in parentheses in Tables S5 and S6) with respect to those of the unsubstituted phenyl compound (**2a** and **3a**, respectively). It can be noted that the influence of the substituent present in the phenyl ring on the signals belonging to the benzimidazole moiety is very low (no more than about 2 ppm). Conversely, as expected, the main chemical shift differences are observed on the signals of the carbon atoms belonging to the phenyl ring. This is a result of the effect of the substituent; the chemical shifts of the carbon atoms in position *ipso* and *ortho* with respect to the substituent are the mainly influenced, especially when a strong electron-withdrawing (nitro) or a strong electron-donating (*N*,*N*-dimethylamino) group is present.

Moreover, by comparing the chemical shifts of the benzimidazole moiety of the two *N*-methyl isomers, it emerges that, for all methylated compounds, the major differences are observed on C-4, C-7, and C-7a but the inversion in chemical shift trend for C-4 and C-7 along the two series is only in apparent discordance, due to the arbitrary numbering adopted. Actually, in current numbering, the azole N=C group can be considered as a *ortho*-substituent to both C-4 for 1-methyl-6-nitrobenzimidazoles and C-7 for 1-methyl-5-nitrobenzimidazoles, thus resonating downfield with respect to C-7 and C-4 of 1-methyl-5-nitrobenzimidazoles (**2**) and 1-methyl-6-nitrobenzimidazoles (**3**), respectively. Analogous consideration might be advanced to explain the downfield shift observed for C-7a of 1-methyl-5-nitrobenzimidazoles.

3.2. NMR data useful for quantitative evaluations

3.2.1. Determination of the tautomeric constants and application of Hammett equation to equilibrium constants

With the aim of determining the tautomeric constant K_T for the equilibrium depicted in Scheme 1 we designed to collect ^{1}H NMR data under conditions in which the signals of the two tautomeric species might appear distinct in the spectrum. Since the exchange equilibrium between the tautomers is temperature-dependent, we carried out a DNMR study to find the suitable conditions to slow down or even to block the prototropic process with the scope of obtaining distinguishable signals for the two species. The spectra were collected –76 °C in acetone d_6 on 10^{-3} M solution for each compound and the data are reported in Table 1.

In all cases, except for the compound **1f**, that precipitated at this concentration, we observed a separation of some signals belonging to the two tautomers, thus measuring the ratio between them and therefore the tautomeric constant. In particular, the NH and H-7 signals were splitted into two separate signals whereas the H-4 signal was sometimes superimposed onto other signals.

In Table 2 are reported the relevant tautomeric ratios, calculated from ^{1}H NMR spectrum, for compounds **1a**–**e**, and the related tautomeric constant. We labelled as tautomer **A** that showing the lower field H-7 signal, without assignment of the structure to each tautomer. However, by a rough comparison of some chemical shifts of the two separate structures with those (see Table S7 in SI) of the two *N*-methyl derivatives (blocked parents) in acetone d_6, it might be deduced that the major tautomer is that with the nitro group in position 6 of the benzimidazole moiety: a behavior that appears in agreement with similar structures reported in the literature (Benassi et al., 1971; Claramunt et al., 2004; Elguero et al., 1976) and that is supported by quantum chemical calculations.

Table 1 ^{1}H NMR data (600 MHz, δ in ppm, *J* in Hz) of 1a-e recorded in acetone d_6 at −76 °C.[a]

Compound	H-4	H-5	H-7	H-2′/H-6′	H-3′/H-5′	H-4′	NH
1a	7.85 (d, *J* = 8.9 Hz, 1H, min.) 7.73 (d, *J* = 8.9 Hz, 1H, maj.)	8.17 (d, *J* = 8.9 Hz, 2H, maj. + min.)	8.56 (d, *J* = 1.9 Hz, 1H, maj.) 8.39 (d, *J* = 1.9 Hz, 1H, min.)	8.29–8.22 (m, 4H)	7.63–7.58 (m)	Overlapped on those of $H_{3'}$ and $H_{5'}$	13.58 (s, 1H, NH min.) 13.42 (s, 1H, NH maj.)
1b	7.84–7.77 (m, 1H, maj. + min.)	8.20 (dd, J_1 = 8.8 Hz, J_2 = 1.7 Hz 1H, maj. + min.)	8.57 (br.s, 1H, maj.)8.46 (v. br.s, 1H, min.)	**H-2′** 8.49 (s, 1H, maj. + min.)**H-6′** 8.23 (d, *J* = 7.9 Hz, 1H, (maj. + min.)	**H-5′** 7.60 (t, *J* = 7.8 Hz, 1H, maj. + min.)	7.81 (d, *J* = 7.9 Hz, 1H, (maj. + min.)	13.45 (v.br.s, 1H, NH min.) 13.31 (br.s, 1H, NH maj.)
1c	7.90–7.72 (m, 1H, maj. + min.)	8.20 (dd, J_1 = 8.7 Hz, J_2 = 2.0 Hz 1H, maj. + min.)	8.57 (br.s, 1H, maj.) 8.45 (v.br.s, 1H, min.)	8.33 (t, *J* = 5.7 Hz, 2H, (maj. + min.)	7.48 (t, *J* = 8.7 Hz, 2H, (maj. + min.)		13.34 (v.br.s, 1H, NH min.) 13.29 (br.s, 1H, NH maj.)
1d	7.88 (d, *J* = 8.8 Hz, 1H, min.) 7.77 (d, *J* = 8.7 Hz, 1H, maj.)	8.20 (dt, J_1 = 8.8 Hz, J_2 = 1.9 Hz 1H, maj. + min.)	8.59 (d, *J* = 1.9 Hz, 1H, maj.) 8.43 (d, *J* = 1.9 Hz, 1H, min.)	8.27 (t, *J* = 8.5 Hz, 2H, maj. + min.)	7.70 (d, *J* = 8.5 Hz, 2H, maj. + min.)		13.50 (s, 1H, NH min.) 13.36 (s, 1H, NH maj.)
1e	7.73 (d, *J* = 9.2 Hz, 1H, min.) 7.66 (d, *J* = 8.9 Hz, 1H, H_4, maj.)	8.14 (t, *J* = 10.0 Hz, 1H, maj. + min.)	8.46 (s, 1H, maj.) 8.30 (s, 1H, min.)	8.09 (t, *J* = 7.2 Hz, 2H, maj. + min.)	6.65 (t, *J* = 7.0 Hz, 2H, maj. + min.)		13.00 (s, 1H, NH min.) 12.92 (s, 1H, NH maj.)

[a] The abbreviations maj and min refer to the signals belonging to the isomer present in the mixture in major or minor amount, respectively.

Table 2 Tautomeric constant for compounds **1a-e** calculated *via* ^{1}H NMR.[a]

Compound (Ar in Scheme 1)	Tautomer 1[b] B[c]	Tautomer 2[b] A[c]	K_T Taut. A/Taut. B
1a Ar = C_6H_5	62.5 ± 0.5	37.5 ± 0.5	0.60 ± 0.01
1b Ar = 3-Br-C_6H_4	66.3 ± 0.3	33.7 ± 0.3	0.508 ± 0.005
1c Ar = 4-F-C_6H_4	62.3 ± 0.7	37.7 ± 0.7	0.61 ± 0.01
1d Ar = 4-Cl-C_6H_4	63.9 ± 0.1	36.1 ± 0.1	0.564 ± 0.002
1e Ar = 4-$(NCH_3)_2$-C_6H_4	53.6 ± 0.4	46.4 ± 0.4	0.87 ± 0.01

[a]600 MHz, acetone d_6, –76 °C. [b] Relative % peak area calculated from ^{1}H NMR spectrum. [c] Attribution based on DFT calculations.

DFT calculations (Fig. 4) confirmed that the most stable tautomer (ΔE = 0.30 kcal mol^{-1}) is characterized by the nitro group in position 6 of the benzimidazole moiety, that is the most abundant tautomer B. This is true for all the compounds **1a–f** (Fig. 5).

It is noteworthy that the K_T values obtained are in agreement with those reported for other benzimidazole derivatives (Benassi et al., 1971; Elguero et al., 1976; Claramunt et al., 2004).

Finally, we tried to see if the substituents present in the 2-aryl group linked to the imidazole ring might 'quantitatively' affect the tautomeric equilibrium by using the Hammett equation. Of course, as the substituent is quite far from the ring involved in the tautomerism (it is on the *para* position of the phenyl ring linked to C-2 of the imidazole ring) we can forecast a low value for the reaction constant (ρ) in the Hammett equation. Accordingly, correlating the experimental K_T *versus* the Hammett parameter σ_p of the substituent we obtained a satisfactory correlation (r^2 0.9967) with a low value for susceptibility constant (ρ-0.171 ± 0.007) in line with expectations. The obtained graphic is shown in Fig. 6.

3.2.2. Application of Hammett equation to variations of ^{13}C chemical shifts of C-1′ and C-2

Moreover, we have examined how the substituents present in the *para*-position of the 2-aryl ring can affect the ^{13}C chemical shifts of C-1′ and of C-2 of the three series of compounds **1**–**3**, by plotting the relevant Δδ versus the Hammett constants (Figs. S1–S6).

Looking at the effect on C-1′, that is on the carbon in *para*-position with respect to the substituents, as expected, in the three series we have observed quite similar and high susceptibility constants (ρ 11.6 for compounds of series **1**; ρ 12.1 and 11.9 for compounds of series **2** and **3**) with satisfactory correlation coefficients ($r^2 \geq 0.993$).

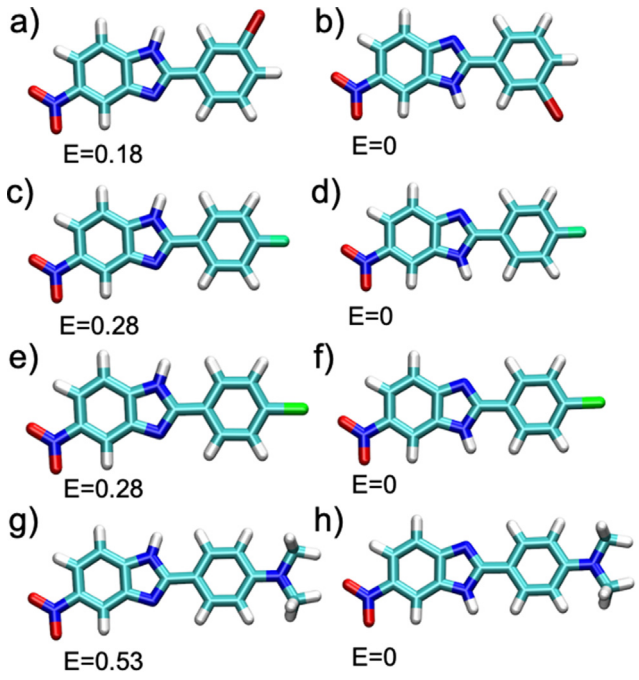

Fig. 5 Optimized structures of 1b [a) and b): Ar = 3-Br-C_6H_4]; 1c [c) and d): Ar = 4-F-C_6H_4]; 1d [e) and f): Ar = 4-Cl-C_6H_4]; 1e [g) and h): Ar = 4-$(NCH_3)_2$-C_6H_4]; a), c), e), g): 5-nitrobenzimidazole tautomer; b), d), f), h): 6-nitrobenzimidazole tautomer.

In line with expectations the effect of the substituents on C-2 is inverted and, of course, much lower. Very similar susceptibility constants have been calculated for compounds of series **2** and **3** (ρ -1.85 - and 1.93, respectively), while for compounds of series **1** once more a constant a little higher (ρ -2.21) has

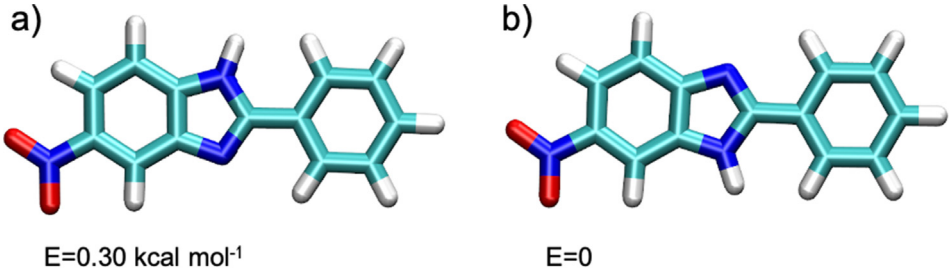

Fig. 4 Optimized structures of a) 2-phenyl-5-nitrobenzimidazole and b) 2-phenyl-6-nitrobenzimidazole.

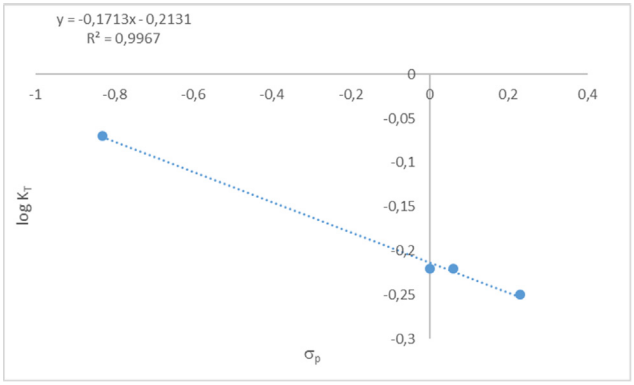

Fig. 6 Plot of K_T *vs.* σ substituent constants.

been observed. Also in these relationships, satisfactory correlation coefficients (r2 $\geq$ 0.992) have been observed.

Interestingly, looking both to the effects of *para*-substituents on ^{13}C chemical shifts of C-1′ and on C-2 we have observed values of the susceptibility constants a little higher in compounds of series **1** than in those of series **2** and **3**, that show very similar effects among themselves.

Of course, all of the obtained results are well in line with literature results (Ewing, 1979) on the effects of substituents on the variations of the ^{13}C chemical shifts in a benzene ring. In fact, a plot of the effect of substituents in **1a**–**f** and in monosubstituted benzenes on ^{13}C chemical shifts give an excellent relationship with unitary slope (see Table S8 and Fig. S7).

3.3. Electrochemical studies

Since we are interested in the reactivity of the nitro group in the benzimidazole moiety, first we describe the electrochemical behavior of series **2** and **3** pointing out the effect of the different substituents on the aryl ring and the possible effect deriving from the presence of a methyl group on a nitrogen atom of the imidazole ring, which generates the two "isomeric" series. In particular, it is interesting to discuss the effect of the nitro group in the aryl ring on the electrochemical behavior of the benzimidazole nitro group. Later, the series **1a**–**f** is taken into account since in such a case the mobile imidazole proton, which is responsible for the prototropic tautomerism, as described in detail above, can react with the nitro radical anion leading to a complex signal in electrochemical characterizations.

3.3.1. Voltammetric behavior of N-methyl-benzimidazoles *2a–f* and *3a–f*

The electrochemical behavior of series **2** and **3** was investigated by cyclic voltammetry in acetonitrile (Fig. 7 and Table S9). All compounds exhibit redox waves in the catho-

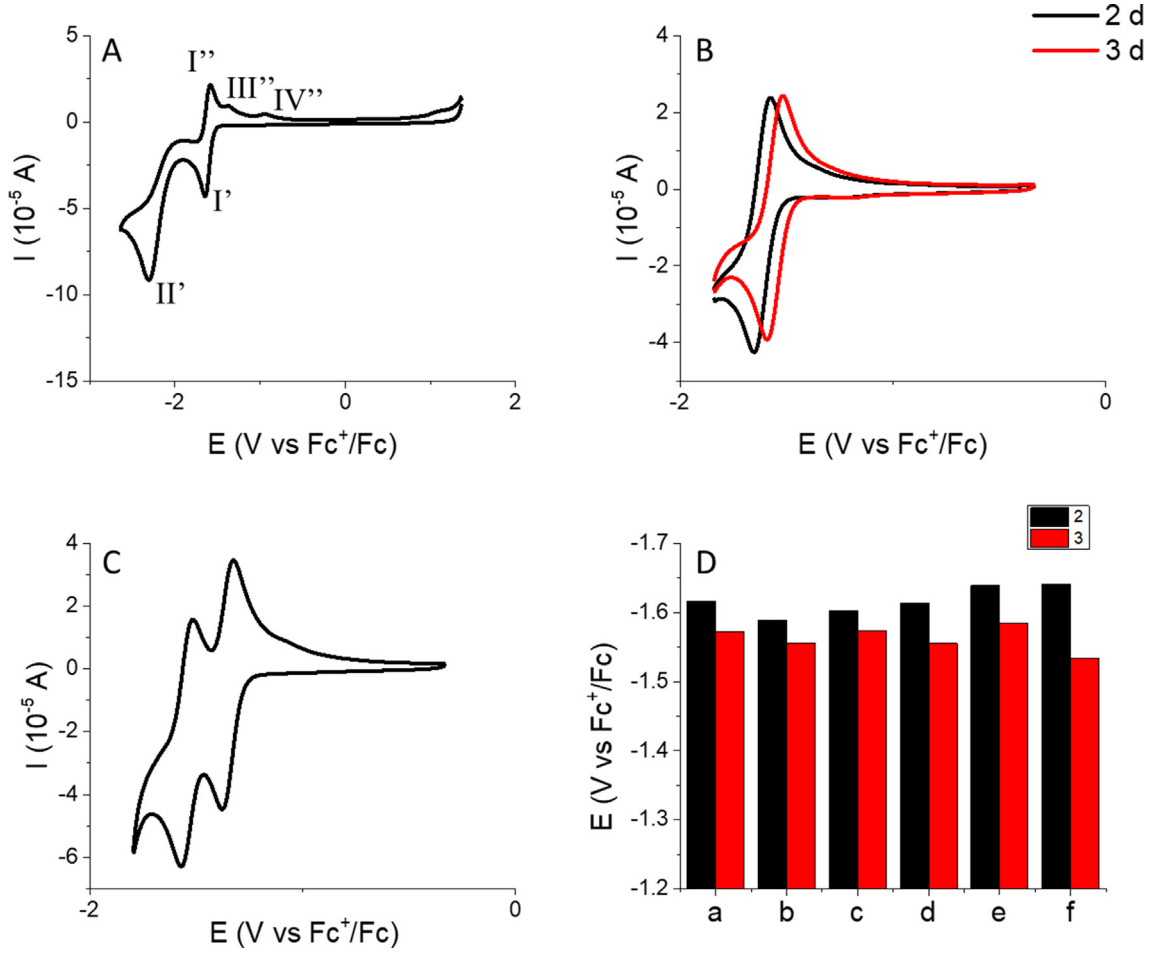

Fig. 7 Cyclic voltammograms of **2a** (A), **2d** and **3d** (B) and **3f** (C) recorded at a scan rate of 0.05 V s^{-1} in acetonitrile. Formal potentials (D) of the benzimidazole nitro group reduction of **2a**–**f** and **3a**–**f**.

dic side, while anodic processes are observed only when the investigated species have an amino group as substituent. The formal potential (E°') was calculated from the half-sum of the cathodic and anodic peak potentials for the reversible processes, while the peak potential is reported for the irreversible waves.

The CVs of **2a–d** and **3a–d** (X = H, 3-Br, 4-F. 4-Cl) series are similar. The CV relevant to compound **2a** is reported in Fig. 7 as example of an electrochemical characterization of **2a–d** and **3a–d** compounds. The process at about –1.6 V (I'/I'') is mono-electronic and is ascribable to the reversible reduction of nitro group to RNO_2^- radical. Since the electrochemical behavior is investigated in an aprotic medium, the reversible generation of the radical anion of a nitro-aromatic compound is the expected reaction. The process at about –2.2 V (II') is irreversible because it is followed by a chemical reaction leading to electroactive species which generate the anodic redox waves at about –1.3 (III'') and –1.0 V (IV''). These waves do not appear in CV response wherein the potential scan is inverted before the occurrence of the irreversible more cathodic process, so highlighting that III'' and IV'' waves are related to the II' wave. Since the II' process leads to a possible molecule degradation, the further discussion on the reactions which take place in the cathodic direction will be focused only on the reduction of nitro group.

Compounds **2e** and **3e** contain the 4-dimethylamino group as substituent at the aryl ring. Their electrochemical properties in the cathodic side are similar to the ones displayed by **2a–d** and **3a–d**, however, three redox processes are present when the anodic potential region is investigated. For both **2e** and **3e** compounds, the first process is quasi reversible with a formal potential of +0.55 V, the second oxidation is reversible and occurs at about +0.80 V, while the third process is irreversible and takes place at about +1.0 V. All these processes are ascribable to the overall multi-electron oxidation of the amino group.

When the cathodic side is examined for **2a–e** and **3a–e**, the potentials of reversible and irreversible processes are slightly affected by the substituent on the aryl group. In addition, also the position of the methyl group does not exert a great effect on these potentials, even if the compounds of series **2** undergo the reduction of nitro group at more cathodic potential than those of series **3** (Fig. 7 C). This evidence is in agreement with the electronic features of the group in *para*-position. Compounds of series **2** have in *para*-position an electron donating 'pyrrole-like' nitrogen, while **3a–f** display an electron attracting 'pyridine-like' nitrogen. Therefore, the reduction is easier for the series **3**, since in such a case the additional electron on nitro group generates a more stable radical anion.

The presence of a nitro substituent on the aryl ring highly affects the CVs of **2f** and **3f** compounds. Two reversible processes occur at about –1.35 V and –1.60 V (Fig. 7 D), that are relevant to the mono-electronic reductions of the nitro group on the aryl ring and of the nitro group of the benzimidazole moiety, respectively. Differently from the couples of compounds **2a–e** and **3a–e** with the same substituent, the position of methyl group does not change the potential of the first reversible reduction process of **2f** or **3f** (–1.353 and –1.351 V, respectively). Therefore, this wave can be surely ascribed to the reduction of the nitro group on the aryl ring. At the same time, the potentials of the second processes depend slightly on the position of the methyl group (–1.641 V for **2f** and –1.534 V for **3f**), and thus it can be assigned to the reduction of the nitro group present on the benzimidazole.

3.3.2. *Voltammetric behavior of NH-benzimidazoles **1a–f***

Table 3 summarizes the electrochemical behavior of compounds **1a–f**.

[a]Red_1, red_2, red_3 and red_4 subscripts indicate the first, second, third and fourth redox processes recorded in the cathodic side for the starting compounds, respectively. Ep and $E^{0\prime}$ indicate peaks and formal potentials, respectively. Rev indicates a reversible process. Irr indicates an irreversible process that could be characterized by a complex kinetics with chemical and electrochemical additional steps.

Analogously to series **2** and **3**, compounds of series **1** exhibit redox waves in the examined range of cathodic potential, while compound **1e** is also electroactive in the anodic region, due to the presence of the dimethylamino group. Fig. 8 shows the CV of **1d** as an example of the electrochemical behavior of the compounds **1a–d**.

The first process occurring in the cathodic direction (I') is irreversible (Ep = –1.4 V), while a second reversible process (II'/II'') takes place at about –1.9 V (E°'). This behavior is in agreement with Roffia's observation concerning 4-nitroimidazoles (Roffia et al., 1982) and with the results obtained by Lopyrev (Lopyrev et al., 1985) who studied the reduction of nitrobenzimidazoles. Both processes are associated to the reduction of nitro group that occurs at different potential because it also involves the acid proton on imidazole ring, which is in sub-stoichiometric amount. The irreversibility of the first peak is due to the quick decay of RNO_2^- radical because of a protonation process (reactions 1–2).

$$HRNO_2 + e^- \rightleftarrows HRNO_2^{-\bullet} \quad (1)$$

$$HRNO_2^{-\bullet} + HRNO_2 \rightarrow HRNO_2H^{\bullet} + RNO_2^{-\bullet} \quad (2)$$

Table 3 Electrochemical properties of nitrobenzimidazoles **1.**[a]

Series **1** 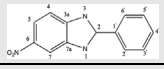	$E_{p,red1}$ (V)/kinetics	$E^0_{red2}{}'$ (V)/Kinetics	$E_{p,red3}$ (V)/kinetics	$E_{p,red4}$ (V)/kinetics
1a	–1.432/irr	–1.908/rev		
1b	–1.361/irr	–1.866/rev		
1c	–1.411/irr	–1.858/rev		
1d	–1.350/irr	–1.866/rev		
1e	–1.476/irr	–1.899/rev		
1f	–1.113/irr	–1.573/rev	–1.829/irr	–1.960/irr

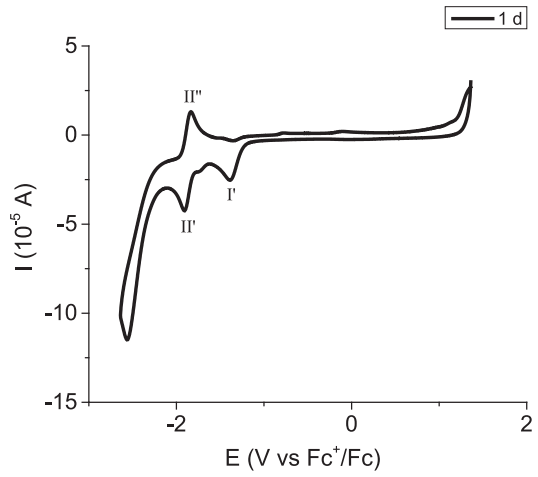

Fig. 8 Cyclic voltammogram of **1d** recorded in acetonitrile at a scan rate of 0.05 V s^{-1}.

Since $HRNO_2H^{\bullet}$ can be in turn reduced at the potential of reaction 1, the redox process continues until the formation of hydroxyl amino derivative with a complex mechanism characterized by several chemical and electrochemical steps. The overall reaction is:

$$5HRNO_2 + 4\,e^- \rightarrow 4\,RNO_2^- + HRNHOH + H_2O \quad (3)$$

The second reversible wave is associated to the reversible reduction of the conjugated base of the starting compound, *i.e.* RNO_2^-. The reduction takes place at a more cathodic potential than I' since the negative charge hinders its reduction in respect to the neutral species.

The reduction potentials recorded for compounds **1a–e** are less cathodic than the corresponding ones of both series **2** and **3**, suggesting that the electron donating inductive effect of methyl group makes more difficult the reduction of the nitro group of the benzimidazole ring. In addition, the chemical reactions occurring after the acquisition of the first electron could be a further driving force that makes easy the reduction in the series **1**.

The electrochemical behavior of **1f** is affected by the presence of the additional nitro group on the phenyl moiety. The CV is very complex and displays four redox waves associated to the reduction of the two nitro groups which takes place in the presence of sub-stoichiometric amount of protons, due to the production of the hydroxylamino derivate from the nitro group present in the phenyl ring which is the first to be reduced.

We think again that the less cathodic wave can be attributed to the reduction of the phenyl nitro group, while the quasi reversible process with E°' of –1.573 V could involve the nitro group on the benzimidazole moiety. The processes occurring at the most cathodic potentials which are irreversible could be ascribed to degradation reactions due to the instability of the relevant dianions. Further voltammograms are reported in Figs. S88-S105 of Supporting Information.

3.4. ESR measurements

In order to evaluate the generation of anion radical species, ESR experiments were performed. The electrochemical reduction in ACN with tetrabuthylammonium perchlorate (0.1 M) as supporting electrolyte, was performed by applying the potential corresponding to reduction peak obtained from the CV experiments, directly inside the cavity of ESR instrument. This procedure proved to be of general applicability for the production of radical anions from 1-methyl-2-aryl-5-nitroben zimidazoles **2a–f** and 1-methyl-2-aryl-6-nitrobenzimidazoles **3a–f**. On the contrary, it was not possible to observe any ESR signal deriving from radical anions of 2-aryl-5-(or 6)-nitrobenzimidazoles (series **1**). This behavior is in agreement with the quick decay of radical anion mediated by proton as previously hypothesized on the basis of CV measurements.

The electrolyzed solution of **2a–f** or **3a–f** displayed in most cases well resolved ESR spectra. As representative examples for the two series, the ESR spectra of **2d** and **3a** are reported in Fig. 9.

All the spectra recorded in ACN were satisfactorily simulated on the basis of the coupling constants reported in Table 4.

Proton assignments to the various positions of nitrobenzimidazoles were attributed by analogy to data reported in the literature on related radical anion species (Ciminale, 2004).

In all cases the ESR spectra are characterized by a nitrogen hyperfine coupling constant, a_N, significantly larger than the coupling constant of any magnetic nucleus belonging to the aryl system of the same radical anion. Since nitroaromatic radical anions generally have most of the spin density localized on

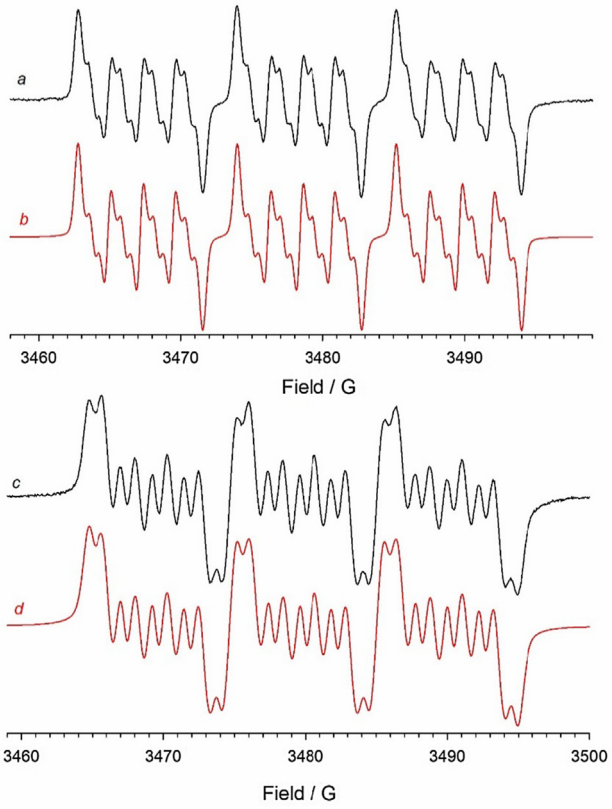

Fig. 9 ESR spectra of the radical species electrogenerated from **2d** (*a*) and **3a** (*c*) in 0.1 M Bu_4NClO_4-ACN. The corresponding theoretical simulations, obtained by using spectroscopic data reported in Table 4, are shown in red (*b*, *d*).

Table 4 Hyperfine coupling constants (in G) of the nitrobenzimidazoles radical anions obtained in ACN by electrochemical reduction.[a]

	a_N (NO_2)	a_{H4}	a_{H5}	a_{H6}	a_{H7}	a_{N1}	a_{N3}	a_H(3′-5′)	a_H(2′-6′)	a_G
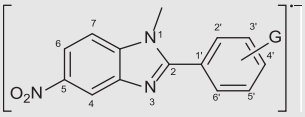										
2a (C_6H_5)	11.31	4.49	–	2.30	0.97	0.37				
2b (3′-Br-C_6H_4)	11.20	4.49	–	2.22	0.96	0.37				
2c (4′-F-C_6H_4)	11.31	4.49	–	2.30	0.95	0.37				
2d (4′-Cl-C_6H_4)	11.23	4.55	–	2.24	0.98	0.36				
2e (4′-(NMe_2)-C_6H_4)	11.44	4.35	–	2.38	0.96	0.31				
2f (4′-NO_2-C_6H_4)						0.49	1.01	3.13	1.05	7.91
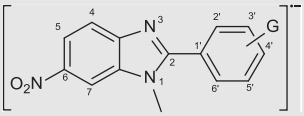										
3a (C_6H_5)	10.30	1.02	2.20	–	4.44	0.61	–	–	–	
3b (3′-Br-C_6H_4)	10.10	1.05	2.16	–	4.54	0.62				
3c (4′-F-C_6H_4)	10.27	0.83	2.14	–	4.38	0.68				
3d (4′-Cl-C_6H_4)	10.23	1.01	2.16	–	4.49	0.64				
3e (4′-(NMe_2)-C_6H_4)	10.56	1.07	2.25	–	4.37	0.54	–	–	–	
3f (4′-NO_2-C_6H_4)						n.d.	0.90	3.05	1.00	7.39

[a] n.d.: not detectable (smaller than line width).

the nitro group (Kolker and Waters, 1964), we could safely conclude that all the spectra obtained from the electrochemical reduction of **2a–e** or **3a–e** are due to the radical anion of substituted nitrobenzimidazoles. The only exception is represented by the two derivatives containing the nitro group also on the 2-phenyl fragment (**2f** and **3f**, G = NO_2). In this case a different coupling pattern of the unpaired electron with nitrogen atom and two groups of two equivalent protons was observed (see Fig. S8), suggesting that spin density is localized on the 2-nitroaryl moiety rather than on nitrobenzimidazole ring. This result strongly supports CV data indicating that reductive processes occurs on the aryl unit when G = NO_2.

DFT calculations confirmed the results obtained by CV and EPR experiments. In fact, the reduction of compounds **2a–e** and **3a–e** leads to radical anions in which the spin densities are mainly localized in the nitrobenzimidazoles, as showed by Fig. 10a and 10b. This process corresponds to the reduction peak observed at about –1.6 V.

On the opposite, in the two compounds containing the nitro group also on the 2-aryl fragment (**2f** and **3f**, Fig. 10c and 10d) following the first reduction process, the spin densities are mainly localized on the nitroaryl moiety, because the reduction of the nitro group on the aryl ring occurs at a lower potential (–1.35 V) than the reduction of the nitro group located on the benzimidazole (–1.60 V). It is in the second reduction process (–1.60 V) of the compounds **2f** and **3f** that the nitro group of the benzimidazole moiety is reduced. Now, the two unpaired electrons (triplet state of the dianion) are localized one in the nitrobenzimidazole ring and one on the nitroaryl ring (Fig. 10e and 10f), as showed by the isosurfaces spin densities.

The nitrogen coupling constant decreases with electron-withdrawing groups and increases with electron-donating groups and this effect is principally due to a polar effect on the electron distribution within the nitro group with very little effect on the spin distribution in the aromatic system (Janzen, 1969). In terms of resonance structures this means that the polar effect of a substituent, X, would influence the relative contribution of structures *A* and *B*, more than the contribution of structure *C* (Fig. 11).

An electron-withdrawing substituent, for example, is expected to decrease a_N because it stabilizes structure *A* (possibly, when in *para*-position, by direct conjugation with the nitrogroup) compared to *B*, thus causing a shift of spin density from the nitrogen to the oxygen atoms. On these bases, the 'pyrrole-like' nitrogen present in compounds **2** at *para*-position (with respect to the nitro group) behaves as donating group leading to larger a_N values in the corresponding radical anions. On the contrary, in compounds **3,** the 'pyridine-like' nitrogen behaves as withdrawing-group leading to *ca.* 1 G smaller a_N values for the analogous radical anions.

The absence of detectable coupling of the unpaired electron with the 2-aryl protons in **2a–e** and **3a–e** derivatives, suggests that spin density must be localized on the nitrobenzimidazoles moiety and a small effect of the G substituent on a_N values should be predicted. However, detectable variations of the nitrogen coupling are observed in both series. Differences are larger in series **3**, where higher spin densities on 2-aryl ring can be predicted on the basis of canonical resonance structures.

On a quantitative basis, a satisfactory Hammett correlation (see Fig. 12) between a_N and σ constants was obtained for series 3 (r^2 = 0.992, ρ = −0.33). Similar results have been observed in series **2** (see Fig. S9 in SI).

4. Conclusion

Looking at the interest on benzimidazoles for their chemical reactivity and for their variegate pharmacological/biological activities we have examined NMR, CV, and ESR behavior of some 2-aryl-5(or 6)-nitrobenzimidazoles (**1**) variously sub-

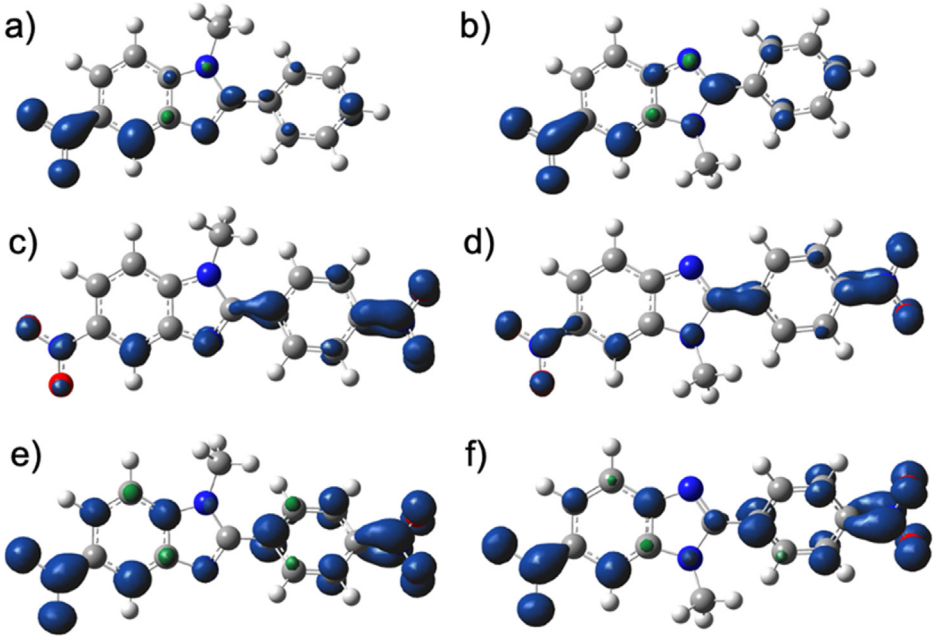

Fig. 10 Isosurfaces spin densities plotted using an isovalue of 0.004 e a_0^{-3} for the radical anion of **2a** (a), **3a** (b), **2f** (c), **3f** (d) and triplet state of the dianion **2f** (e), **3f** (f). Images created with GaussView 6.

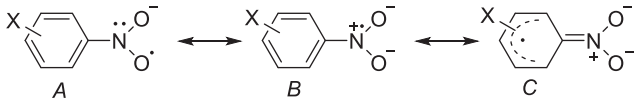

Fig. 11 Main resonance structures for substituted nitrobenzene radical anions.

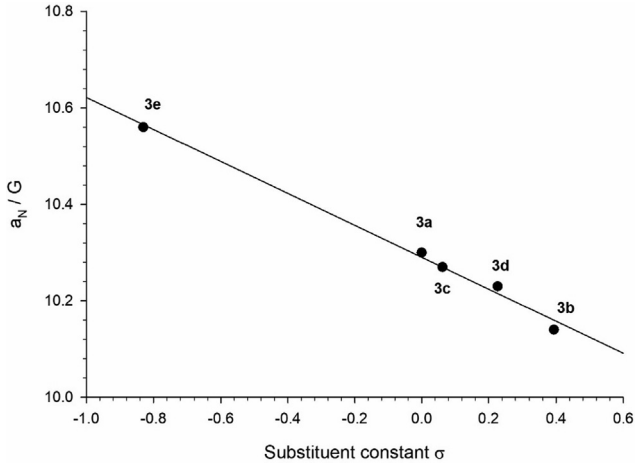

Fig. 12 Plot of a_N *vs.* σ substituent constants for compounds of series **3**.

stituted in the 2-aryl ring and of their N-methyl derivatives (1-methyl-2-aryl-5-nitrobenzimidazoles, **2**, and 1-methyl-2-aryl-6-nitrobenzimidazoles, **3**).

Thus, by using ^{1}H NMR data we have been able to study the equilibrium between the tautomers **1A** and **1B**, also calculating the relevant equilibrium constants, whose values have been correlated with the effect of the present substituent. A deep investigation of the ^{13}C NMR data has allowed a quantitative evaluation of the effects of the substituents present in 2-aryl ring on C-1′ and on C-2 chemical shifts, evidencing that they show similar effects in the three classes of compounds.

As to the electrochemical behavior of the nitro group of the benzimidazole ring (**2** and **3** series) the mono-electronic process can be considered always reversible and little affected by the substituents present on the aryl ring with the exception of the nitro group. In such a case both the nitro groups undergo a reversible reduction but the one present on the aryl ring occurs at a much less cathodic potential. These results were supported by ESR measurements on the corresponding radical anions. As far as the series **1** is concerned, the reduction potentials are less cathodic than the corresponding ones of both series **2** and **3**, and the electrochemical behavior of the nitro group of the benzimidazole ring is strongly influenced by the presence of the mobile proton on the N atom of the imidazole ring. In such a case, a further irreversible reduction involving more electrons and protons to produce the hydroxylamino derivative takes place.

All the obtained data have been supported by DFT calculations.

Therefore, in the whole, we can say that the obtained data have been able to give deep information on the electronic distribution of the three classes of examined compounds (**1**–**3**) allowing us to gain a picture of electronic distribution and of behavior of the studied benzimidazoles.

CRediT authorship contribution statement

El Mostapha Rakib: Synthesis of compounds **1-3** and writing of introduction. **Carla Boga:** NMR data collection and discussion. **Matteo Calvaresi:** DFT calculations and discussion. **Mohamed Chigr:** Synthesis of compounds **1-3**. **Paola Franchi:**

ESR data collection and writing.**Isacco Gualandi:** CV data collection and writing. **Aziz Ihammi:** synthesis of compounds **1-3**. **Marco Lucarini:** ESR data discussion. **Gabriele Micheletti:** NMR data collection and discussion. **Domenico Spinelli:** Coordination of all activities, discussion, supervising and writing the paper. **Domenica Tonelli:** CV data discussion and financial support

Declaration of Competing Interest

The authors declare that they have no known competing financial interests or personal relationships that could have appeared to influence the work reported in this paper.

Acknowledgments

Work supported by Alma Mater Studiorum – Università di Bologna (RFO funds).

Appendix A. Supplementary material

Supplementary data to this article can be found online at https://doi.org/10.1016/j.arabjc.2021.103179.

References

Alberti, A., Benaglia, M., Hapiot, P., Hudson, A., Le Coustumer, G., Macciantelli, D., Masson, S., 2000. Phosphoryl- and thiophosphoryl-dithioformates. Part IV. Electrochemical reduction and EPR study of the radical anions. J. Chem. Soc Perkin Trans. 2, 1908–1913. https://doi.org/10.1039/b002986f.

Bahrami, K., Khodaei, M.M., Kavianinia, I., 2007. A simple and efficient one-pot synthesis of 2-substituted benzimidazoles. Synthesis 547–550. https://doi.org/10.1055/s-2007-965878.

Bansal, Y., Silakari, O., 2012. The therapeutic journey of benzimidazoles. Bioorg. Med. Chem. 20, 6208–6236. https://doi.org/10.1016/j.bmc.2012.09.013.

Beaulieu, P.L., Hache, B., von Moos, E.A., 2003. Practical oxone-mediated, high-throughput, solution-phase synthesis of benzimidazoles from 1,2-phenylenediamines and aldehydes and its application to preparative scale synthesis. Synthesis 11, 1683–1692. https://doi.org/10.1055/s-2003-40888.

Benassi, R., Lazzeretti, P., Schenetti, L., Taddei, F., Vivarelli, P., 1971. NMR study of tautomerism in substituted 2-chlorobenzimidazoles. Tetrahedron Lett. 12, 3299–3300. https://doi.org/10.1016/S0040-4039(01)97160-6.

Becke, A.D., 1993. Density-functional thermochemistry. III. The role of exact exchange. J. Chem. Phys. 98, 5648–5652. https://doi.org/10.1063/1.464913.

Bhattacharya, S., Chaudhuri, P., 2008. Medical implications of benzimidazole derivatives as drugs designed for targeting DNA and DNA associated processes. Curr. Med. Chem. 15, 1762–1777. https://doi.org/10.2174/092986708785133013.

Bianchi, L., Dell'Erba, C., Maccagno, M., Morganti, S., Petrillo, G., Rizzato, E., Sancassan, F., Severi, E., Spinelli, D., Tavani, C., 2006. Nitrobutadienes from β-nitrothiophenes: valuable building-blocks in the overall ring-opening/ring-closure protocol to homo- or hetero-cycles. Arkivoc 7, 169–185. https://doi.org/10.3998/ark.5550190.0007.714.

Bird, C.W., 1992. Heteroaromaticity, 5, a unified aromaticity index. Tetrahedron 48, 335–340. https://doi.org/10.1016/S0040-4020(01)88145-X.

Boga, C., Calvaresi, M., Franchi, P., Lucarini, M., Fazzini, S., Spinelli, D., Tonelli, D., 2012. Electron reduction processes of nitrothophenes. A systematic approach by DFT computations, cyclic voltammetry and E-ESR spectroscopy. Org. Biomol. Chem. 10, 7986–7995. https://doi.org/10.1039/c2ob26128f.

Boga, C., Micheletti, G., Cino, S., Fazzini, S., Forlani, L., Zanna, N., Spinelli, D., 2016a. C-C coupling between trinitrothiophenes and triaminobenzenes: zwitterionic intermediates and new all-conjugated structures. Org. Biomol. Chem. 14, 4267–4275. https://doi.org/10.1039/c6ob00243a.

Boga, C., Cino, S., Micheletti, G., Padovan, D., Prati, L., Mazzanti, A., Zanna, N., 2016b. New azo-decorated N-pyrrolidinylthiazoles: synthesis, properties and an unexpected remote substituent effect transmission. Org. Biomol. Chem. 14, 7061–7068. https://doi.org/10.1039/c6ob00994h.

Budriesi, R., Cosimelli, B., Ioan, P., Lanza, C.Z., Spinelli, D., Chiarini, A., 2002. Cardiovascular characterization of [1,4]thiazino[3,4-*c*][1,2,4]oxadiazol-1-one derivatives: selective myocardial calcium channel modulators. J. Med. Chem. 45, 3475–3481. https://doi.org/10.1021/jm020815d.

Carosati, E., Cosimelli, B., Ioan, P., Severi, E., Katneni, K., Chiu, F.C.K., Saponara, S., Fusi, F., Frosini, M., Matucci, R., Micucci, M., Chiarini, A., Spinelli, D., Budriesi, R., 2016. Understanding oxadiazolothiazinone biological properties: negative inotropic activity versus cytochrome P450-mediated metabolism. J. Med. Chem. 59, 3340–3352. https://doi.org/10.1021/acs.jmedchem.6b00030.

Chen, Y.X., Qian, L.F., Zhang, W., Han, B., 2008. Efficient aerobic oxidative synthesis of 2-substituted benzoxazoles, benzothiazoles, and benzimidazoles catalyzed by 4-methoxy-TEMPO. Angew. Chem. Int. Ed. 47, 9330–9333. https://doi.org/10.1002/anie.200803381.

Ciminale, F., 2004. Radical anions of nitrobenzothiazoles: EPR study of conjugative properties of benzothiazolyl systems. Tetrahedron Lett. 45, 5849–5852. https://doi.org/10.1016/j.tetlet.2004.06.004.

Claramunt, R.M., López, C., Alkorta, I., Elguero, J., Yang, R., Schulman, S., 2004. The tautomerism of Omeprazole in solution: a ^{1}H and ^{13}C NMR study. Magn. Reson. Chem. 42, 712–714. https://doi.org/10.1002/mrc.1409.

Claramunt, R.M., López, C., Santa María, M.D., Sanz, D., Elguero, J., 2006. The use of NMR spectroscopy to study tautomerism. Prog. Nucl. Magn. Reson. Spectrosc. 49, 169–206. https://doi.org/10.1016/j.pnmrs.2006.07.001.

Cuviello, F., Cosimelli, B., Armentano, M.F., Bufo, S.A., Bisaccia, F., Spinelli, D., Ostuni, A., 2019. The P-glycoprotein inhibitor diltiazem-like 8-(4-chlorophenyl)-5-methyl-8-[(2Z)-pent-2-en-1-yloxy]-8H-[1,2,4]oxadiazolo[3,4-*c*][1,4]thiazin-3-one inhibits esterase activity and H3 histone acetylation. Eur. J. Med. Chem. 164, 1–7. https://doi.org/10.1016/j.ejmech.2018.12.037.

Das, K., Mondal, A., Srimani, D., 2018. Selective synthesis of 2-substituted and 1,2-disubstituted benzimidazoles directly from aromatic diamines and alcohols catalyzed by molecularly defined nonphosphine manganese(I) complex. J. Org. Chem. 83, 9553–9560. https://doi.org/10.1021/acs.joc.8b01316.

D'Anna, F., Frenna, V., Macaluso, G., Marullo, S., Morganti, S., Pace, V., Spinelli, D., Spisani, R., Tavani, C., 2006. On the rearrangement in dioxane/water of (*Z*)-arylhydrazones of 5-amino-3-benzoyl-1,2,4-oxadiazole into (2-aryl-5-phenyl-2h-1,2,3-triazol-4-yl)ureas: substituent effects on the different reaction pathways. J. Org. Chem. 71, 5616–5624. https://doi.org/10.1021/jo0605849.

Dell'Erba, C., Spinelli, D., 1965. Thiophene series – VI: Substituent effect on the rate of nucleophilic substitution: kinetics of the reaction between 2-bromo-3-nitro-5-X-thiophenes and piperidine in ethanol. Tetrahedron 21, 1061–1066. https://doi.org/10.1016/0040-4020(65)80046-1.

Dell'Erba, C., Mele, A., Novi, M., Petrillo, G., Sancassan, F., Spinelli, D., 1990. On the nature of resonance interactions in substituted benzenes. Part 3. A 13C nuclear magnetic resonance study of substituent effects in 4-substituted benzamides and methyl ben-

zoates in dimethyl sulphoxide. J. Chem. Soc. Perkin Trans. 2, 2055–2058. https://doi.org/10.1039/p29900002055.

Delpivo, C., Micheletti, G., Boga, C., 2013. A green synthesis of quinoxalines and 2,3-dihydropyrazines. Synthesis 45, 1546–1552. https://doi.org/10.1055/s-0033-1338441.

Del Vecchio, E., Boga, C., Forlani, L., Tozzi, S., Micheletti, G., Cino, S., 2015. Ring closure of azo compounds to 1,2-annulated benzimidazole derivatives and further evidence of reversibility of the azo coupling reaction. J. Org. Chem. 80, 2216–2222. https://doi.org/10.1021/jo5027244.

Desai, K.G., Desai, K.R., 2006. Green route for the heterocyclization of 2-mercaptobenzimidazole into beta-lactum segment derivatives containing -CONH- bridge with benzimidazole: Screening in vitro antimicrobial activity with various microorganisms. Bioorg. Med. Chem. 14, 8271–8279. https://doi.org/10.1016/j.bmc.2006.09.017.

El-Gohary, N.S., Shaaban, M.I., 2017. Synthesis and biological evaluation of a new series of benzimidazole derivatives as antimicrobial, antiquorum sensing and antitumor agents. Eur. J. Med. Chem. 131, 255–262. https://doi.org/10.1016/j.ejmech.2017.03.018.

Elguero, J., Marzin, C., Katritzky, A.R., Linda, P., 1976. The Tautomerism of Heterocycles. Academic Press, New York.

El-Karim, S.S.A., Anwar, M.M., Zaki, E.R., Elseginy, S.A., Nofal, Z. M., 2018. Synthesis and molecular modeling of new benzimidazoles as glutathione S-transferase inhibitors and anticancer agents. Future Med. Chem. 10, 157–181. https://doi.org/10.4155/fmc-2017-0137.

Ewing, D.E., 1979. 13C substituent effects in monosubstituted benzenes. Org. Magn. Res. 12, 499–524. https://doi.org/10.1002/mrc.1270120902.

Frenna, V., Lo Meo, P., Palumbo Piccionello, A., Spinelli, D., 2019. Unexpected substituent effects in the iso-heterocyclic boulton-katritzky rearrangement of 3-aroylamino-5-methyl-1,2,4-oxadiazoles: a mechanistic study. J. Phys. Chem. A 123, 10004–10010. https://doi.org/10.1021/acs.jpca.9b08675.

Frisch, M.J., Pople, J.A., Binkley, J.S., 1984. Self-consistent molecular orbital methods 25. Supplementary functions for Gaussian basis sets. J. Chem. Phys. 80, 3265–3269. https://doi.org/10.1063/1.447079.

Frisch, M.J., Trucks, G.W., Schlegel, H.B., Scuseria, G.E., Robb, M. A., Cheeseman, J.R., Scalmani, G., Barone, V., Petersson, G.A., Nakatsuji, H., Li, X., Caricato, M., Marenich, A.V., Bloino, J., Janesko, B.G., Gomperts, R., Mennucci, B., Hratchian, H.P., Ortiz, J.V., Izmaylov, A.F., Sonnenberg, J.L., Williams-Young, D., Ding, F., Lipparini, F., Egidi, F., Goings, J., Peng, B., Petrone, A., Henderson, T., Ranasinghe, D., Zakrzewski, V.G., Gao, J., Rega, N., Zheng, G., Liang, W., Hada, M., Ehara, M., Toyota, K., Fukuda, R., Hasegawa, J., Ishida, M., Nakajima, T., Honda, Y., Kitao, O., Nakai, H., Vreven, T., Throssell, K., Montgomery Jr., J. A., Peralta, J.E., Ogliaro, F., Bearpark, M.J., Heyd, J.J., Brothers, E.N., Kudin, K.N., Staroverov, V.N., Keith, T.A., Kobayashi, R., Normand, J., Raghavachari, K., Rendell, A.P., Burant, J.C., Iyengar, S.S., Tomasi, J., Cossi, M., Millam, J.M., Klene, M., Adamo, C., Cammi, R., Ochterski, J.W., Martin, R.L., Morokuma, K., Farkas, O., Foresman, J.B., Fox, D.J., 2016. Gaussian 16, Revision C.01. Gaussian Inc, Wallingford CT.

Gaba, M., Singh, D., Singh, S., Sharma, V., Gaba, P., 2010. Synthesis and pharmacological evaluation of novel 5-substituted-1-(phenylsulfonyl)-2-methylbenzimidazole derivatives as anti-inflammatory and analgesic agents. Eur. J. Med. Chem. 45, 2245–2249. https://doi.org/10.1016/j.ejmech.2010.01.067.

Gualandi, L., Mezzina, E., Franchi, P., Lucarini, M., 2016. Nitroxide radical spin probes for exploring halogen-bonding interactions in solution. Chem. Eur. J. 22, 16017–16021. https://doi.org/10.1002/chem.201603394.

Guven, O.O., Erdogan, T., Goker, H., Yıldız, S., 2007. Synthesis and antimicrobial activity of some novel phenyl and benzimidazole substituted benzyl ethers. Bioorg. Med. Chem. Lett. 17, 2233–2236. https://doi.org/10.1016/j.bmcl.2007.01.061.

Hadole, C., Rajput, J., Bendre, R., 2018. Concise on some biologically important 2-substituted benzimidazole derivatives. Org. Chem. Curr. Res. 7, No.1000195. https://doi.org/10.4172/2161−0401.1000195, DOI: 10.4172/2161-0401.1000195.

Hansch, C., Leo, A., 1979. Substituent Constants for Correlation Analysis in Chemistry and Biology. Wiley-Interscience, NY.

Jain, A., Sharma, R., Chaturvedi, S.C., 2013. A rational design, synthesis, characterization, and antihypertensive activities of some new substituted benzimidazoles. Med. Chem. Res. 22, 4622–4632. https://doi.org/10.1007/s00044-012-0462-7.

Janzen, E.G., 1969. Substituent effects on electron spin resonance spectra and stability of free radicals. Acc. Chem. Res. 279–288. https://doi.org/10.1021/ar50021a004.

Kahveci, B., Yılmaz, F., Menteşe, E., Özil, M., Karaoğlu, Ş.A., 2014. Microwave-assisted synthesis of some novel benzimidazole derivatives containing imine function and evaluation of their antimicrobial activity. J. Heterocycl. Chem. 51, 982–990. https://doi.org/10.1002/jhet.1593.

Kalalbandi, V.K.A., Seetharamappa, J., Katrahalli, U., Bhat, K.G., 2014. Synthesis, crystal studies, anti-tuberculosis and cytotoxic studies of 1-[(2E)-3-phenylprop-2-enoyl]-1H-benzimidazole derivatives. Eur. J. Med. Chem. 79, 194–202. https://doi.org/10.1016/j.ejmech.2014.04.017.

Kolker, P.L., Waters, W.A., 1964. The radical-anions of para-substituted aromatic nitro-compounds. J. Chem. Soc. 1136–1141. https://doi.org/10.1039/JR9640001136.

Kouakou, A., Micheletti, G., Boga, C., Calvaresi, M., Chicha, H., Franchi, P., Guadagnini, L., Lucarini, M., Rakib, E.M., Spinelli, D., Tonelli, D., 2015. Spectroscopic and electrochemical properties of 1- or 2-alkyl substituted 5- and 6-nitroindazoles. Curr. Org. Chem. 19, 1526–1537. https://doi.org/10.2174/1385272819666150615234549.

Kubo, K., Inada, Y., Kohara, Y., Sugiura, Y., Ojima, M., Itoh, K., Furukawa, Y., Nishikawa, K., Naka, T., 1993. Nonpeptide angiotensin II receptor antagonists. Synthesis and biological activity of benzimidazoles. J. Med. Chem. 36, 1772–1784. https://doi.org/10.1021/jm00064a011.

Largeron, M., Nguyen, K.M.H., 2018. Recent advances in the synthesis of benzimidazole derivatives from the oxidative coupling of primary amines. Synthesis 50, 241–253. https://doi.org/10.1055/s-0036-1590915.

Lee, C., Yang, W., Parr, R.G., 1988. Development of the Colle-Salvetti correlation-energy formula into a functional of the electron density. Phys. Rev. B 37, 785–789. https://doi.org/10.1103/PhysRevB.37.785.

Lopyrev, V.A., Larina, L.I., Sosonkin, I.M., Vakul'skaya, T.I., Kalb, G.L., Shibanova, E.F., 1985. EPR and polarography of nitroazoles. 5. First step in the electrochemical reduction of 2-substituted 5(6)-nitrobenzimidazole using a rotating platinum ring-disk electrode. Chem. Heterocycl. Compd. 21, 688–692. https://doi.org/10.1007/BF00515074.

Madkour, H.M.F., Farag, A.A., Ramses, S.S., Ibrahiem, N.A.A., 2006. Synthesis and fungicidal activity of new imidazoles from 2-(chloromethyl)-1H-benzimidazole. Phosphorus Sulfur Silicon Relat Elem 181, 255–265. https://doi.org/10.1080/104265090970241.

Marinescu, M., 2019. Chemistry and Applications of Benzimidazole and its Derivatives. IntechOpen, London.

Mavrova, A.T., Anichina, K.K., Vuchev, D.I., Tsenov, J.A., Denkova, P.S., Kondeva, M.S., Micheva, M.K., 2006. Antihelminthic activity of some newly synthesized 5(6)-(un)substituted-1H-benzimidazol-2-ylthioacetylpiperazine derivatives. Eur. J. Med. Chem. 41, 1412–1420. https://doi.org/10.1016/j.ejmech.2006.07.005.

Micheletti, G., Boga, C., Pafundi, M., Pollicino, S., Zanna, N., 2016. New electron-donor and -acceptor architectures from benzofurazans and sym-triaminobenzenes: intermediates, products and an unusual nitro group shift. Org. Biomol. Chem. 14, 768–776. https://doi.org/10.1039/c5ob02180d.

Micheletti, G., Kouakou, A., Boga, C., Franchi, P., Calvaresi, M., Guadagnini, L., Lucarini, M., Rakib, E.M., Spinelli, D., Tonelli, D., Forsal, I., 2017. Comparative spectroscopic and electrochemical study of N-1 or N-2-alkylated 4-nitro and 7-nitroindazoles. Arab. J. Chem. 10, 823–836. https://doi.org/10.1016/j.arabjc.2016.05.005.

Micheletti, G., Frenna, V., Macaluso, G., Boga, C., Spinelli, D., 2019. Mononuclear rearrangement of the *Z*-Phenylhydrazones of Some 3-Acyl-1,2,4-oxadiazoles: Effect of substituents on the nucleophilic character of the $>C{=}N{-}NH{-}C_6H_5$ chain and on the charge density of N-2 of the 1,2,4-oxadiazole ring (electrophilic counterpart). J. Org. Chem. 84, 2462–2469. https://doi.org/10.1021/acs.joc.8b02305.

Morningstar, M.L., Roth, T., Farnsworth, D.W., Smith, M.K., Watson, K., Buckheit, R.W., Das, J.K., Zhang, W., Arnold, E., Julias, J.G., Hughes, J.S.H., Michejda, C.J., 2007. Synthesis, biological activity, and crystal structure of potent nonnucleoside inhibitors of HIV-1 reverse transcriptase that retain activity against mutant forms of the enzyme. J. Med. Chem. 50, 4003–4015. https://doi.org/10.1021/jm060103d.

Niet, C.I., Cabildo, P., Ángeles García, M., Claramunt, R.M., Alkorta, I., Elguero, J., 2014. An experimental and theoretical NMR study of NH-benzimidazoles in solution and in the solid state: proton transfer and tautomerism. Beilstein J. Org. Chem. 10, 1620–1629. https://doi.org/10.3762/bjoc.10.168.

Panda, S.S., Malik, R., Jain, S.C., 2012. Synthetic approaches to 2-arylbenzimidazoles: a review. Curr. Org. Chem. 16, 1905–1919. https://doi.org/10.2174/138527212802651232.

Pathan, N.B., Rahatgaonkar, A.M., 2016. Solid supported microwave induced synthesis of imidazole–pyrimidine hybrids: Antimicrobial evaluation and docking study as 14DM-CPY51 inhibitors. Arab. J. Chem. 9, 100–108. https://doi.org/10.1016/j.arabjc.2011.02.013.

Perez-Villanueva, J., Hernandez-Campos, A., Yepez-Mulia, L., Mendez-Cuesta, C., Mendez-Lucio, O., Hernandez-Luis, F., Castillo, R., 2013. Synthesis and antiprotozoal activity of novel 2-{[2-(1H-imidazol-1-yl)ethyl]sulfanyl}-1H-benzimidazole derivatives. Bioorg. Med. Chem. Lett. 23, 4221–4224. https://doi.org/10.1016/j.bmcl.2013.05.012.

Pieroni, M., Tipparaju, S.K., Lun, S., Song, Y., Sturm, A.W., Bishai, W.R., Kozikowski, A.P., 2011. Pyrido[1,2-*a*]benzimidazole-based agents active against tuberculosis (TB), multidrug-resistant (MDR) TB and extensively drug-resistant (XDR) TB. ChemMedChem 6, 334–342. https://doi.org/10.1002/cmdc.201000490.

Preston, P. N. 1981 Chem. Heterocycl. Compd.; Weissberger, A., Taylor, E. C., Eds.; John Wiley and Sons: New York, Vol. 40.

Roffia, S., Gottardi, C., Vianello, E., 1982. Electrochemical behaviour of 4-nitroimidazole and 2-methyl-5-nitroimidazole: Autoprotonation of anion radical and redox-catalysed reduction of the supporting electrolyte cation. J. Electroanal. Chem. 142, 263–275. https://doi.org/10.1016/S0022-0728(82)80020-X.

Romagnoli, C., Prati, F., Benassi, R., Orteca, G., Saladini, M., Ferrari, E., 2017. Synthesis, characterization and metal coordination of a potential b-lactamase inhibitor: 5-Methyl-2-phenoxymethyl-3-H-imidazole-4-carboxylic acid (PIMA). Arab. J. Chem. 10, 1061–1069. https://doi.org/10.1016/j.arabjc.2015.11.007.

Rosano, C., Viale, M., Cosimelli, B., Severi, E., Gangemi, R., Ciogli, A., de Todero, D., Spinelli, D., 2013. ABCB1 structural models, molecular docking, and synthesis of new oxadiazolothiazin-3-one inhibitors. ACS Med. Chem. Lett. 4, 694–698. https://doi.org/10.1021/ml300436x.

Shaharyar, M., Abdullah, M.M., Bakht, M.A., Majeed, J., 2010. Pyrazoline bearing benzimidazoles: search for anticancer agent. Eur. J. Med. Chem. 45, 114–119. https://doi.org/10.1016/j.ejmech.2009.09.032.

Shahid, H.A., Jahangir, S., Yousuf, S., Hanif, M., Sherwani, S.K., 2016. Synthesis, crystal structure, structural characterization and in vitro antimicrobial activities of 1-methyl-4-nitro-1H-imidazole. Arab. J. Chem. 9, 668–675. https://doi.org/10.1016/j.arabjc.2014.11.001.

Sondhi, S.M., Singh, N., Kumar, A., Lozach, O., Meijer, L., 2006. Synthesis, anti-inflammatory, analgesic and kinase (CDK-1, CDK-5 and GSK-3) inhibition activity evaluation of benzimidazole/benzoxazole derivatives and some Schiff's bases. Bioorg. Med. Chem. 14, 3758–3765. https://doi.org/10.1016/j.bmc.2006.01.054.

Spinelli, D., Guanti, G., Dell'Erba, C., 1972. Transmission of substituent effects in systems with bonds of different order. Kinetics of the reactions of 3-bromo-2-nitro-4-X-thiophens and 3-bromo-4-nitro-2-X-thiophens with sodium benzenethiolate in methanol. J. Chem. Soc. Perkin Trans. 2, 441–445. https://doi.org/10.1039/p29720000441.

Spinelli, D., Consiglio, G., Noto, R., Corrao, A., 1975. Linear free energy *ortho*-correlations in the thiophen series. Part I. The kinetics of piperidinodebromination of some 2-bromo-3-X-5-nitrothiophens in methanol. J. Chem. Soc. Perkin Trans. 2, 620–622. https://doi.org/10.1039/P29750000620.

Spinelli, D., Zanirato, P., 1993. On the chemical, NMR and kinetic properties of 2-azido- and 3-azidothiophene: recent developments. J. Chem. Soc. Perkin Trans. 2, 1129–1133. https://doi.org/10.1039/p29930001129.

Starčević, K., Kralj, M., Ester, K., Sabol, I., Grce, M., Pavelić, K., Karminski-Zamola, G., 2007. Synthesis, antiviral and antitumor activity of 2-substituted-5-amidino-benzimidazoles. Bioorg. Med. Chem. 15, 4419–4426. https://doi.org/10.1016/j.bmc.2007.04.032.

Stephens, F.F., Bower, J.D., 1949. The preparation of benzimidazoles and benzoxazoles from Schiff's bases. Part I. J. Chem. Soc. 2971–2972. https://doi.org/10.1039/JR9490002971.

Thimmegowda, N.R., Nanjunda Swamy, S., Ananda Kumar, C.S., Sunil Kumar, Y.C., Chandrappa, S., Yip, G.W., Rangappa, K.S., 2008. Synthesis, characterization and evaluation of benzimidazole derivative and its precursors as inhibitors of MDA-MB-231 human breast cancer cell proliferation. Bioorg. Med. Chem. Lett. 18, 432–435. https://doi.org/10.1016/j.bmcl.2007.08.078.

Viale, M., Cordazzo, C., Cosimelli, B., de Todero, D., Castagnola, P., Aiello, C., Severi, E., Petrillo, G., Cianfriglia, M., Spinelli, D., 2009. Inhibition of MDR1 activity in vitro by a novel class of diltiazem analogues: toward new candidates. J. Med. Chem. 52, 259–266. https://doi.org/10.1021/jm801195k.

Vijesh, A.M., Isloor, A.M., Telkar, S., Arulmoli, T., Fun, H.-K., 2013. Molecular docking studies of some new imidazole derivatives for antimicrobial properties. Arab. J. Chem. 6, 197–204. https://doi.org/10.1016/j.arabjc.2011.10.007.

Zhu, Z., Lippa, B., Drach, J.C., Townsend, L.B., 2000. Design, synthesis, and biological evaluation of tricyclic nucleosides (dimensional probes) as analogues of certain antiviral polyhalogenated benzimidazole ribonucleosides. J. Med. Chem. 43, 2430–2437. https://doi.org/10.1021/jm990290y.